International Journal of Nanoelectronics and Materials
Volume 13 (Special Issue) Dec 2020 [75-82]

Effect of Water Molecules Toward the Structural and Electronic Properties of Prussian Blue Cathode Material for Potassium Battery: A First Principles Investigation

Fatin Nabilah Sazman[1], Noor Atiqah Md Nasir[1], Fadhlul Wafi Badrudin[2*], Shahrul Izwan Ahmad[2], Mohamad Fariz Mohamad Taib[1,4*] and Muhd Zu Azhan Yahya[3,4]

[1]*Faculty of Applied Sciences, Universiti Teknologi MARA (UiTM), 40450 Shah Alam, Selangor, Malaysia.*
[2]*Centre for Defence Foundation Studies, Universiti Pertahanan Nasional Malaysia, 57000 Kuala Lumpur.*
[3]*Faculty of Defence Science and Technology, Universiti Pertahanan Nasional Malaysia, 57000, Kuala Lumpur, Malaysia.*
[4]*Ionic Materials & Devices (IMADE) Research Laboratory, Institute of Science, Universiti Teknologi MARA (UiTM), 40450 Shah Alam, Selangor, Malaysia.*

ABSTRACT

$Fe(CN)_6$ vacancies will usually form in the process of Prussian Blue synthetization due to rapid precipitation then will be occupied by water (H_2O) molecules. Through first principles calculation, this situation is simulated and the effect of water H_2O molecules toward the electronic and structural properties are reported and discussed. In these theoretical calculations, the structural properties and electronic properties of pure PB and hydrated PB have been analysed by using density functional theory (DFT). Based on density functional theory (DFT), generalized gradient approximation (GGA-PBE) and GGA+U were used as exchange correlation functionals. As the result, bandgap for GGA-PBE+U was obtained 1.66 eV for pure Prussian Blue (PB). The defect and water molecules were found to influence on the bandgap and density of state of this material and 1.033 eV bandgap were obtained. Base on the lattice parameter, the structure of hydrated PB are shrinking and distorted from the ideal cubic. The structure is weakened as the bond order (BO) for the Fe-N drop about half of the original value.

Keywords: Bond Order, Cathode Material, Defect, First Principles, Potassium-Ion Battery, Prussian Blue, Vacancy, Water Molecules

1. INTRODUCTION

In 18th century, an ancient dye called Prussian Blue (PB) has been invented and recently received attention particularly as alternative cathode material for rechargeable battery. This is due to its rigid and open framework which allow for three-dimensional ion pathway, fast intercalation kinetics and two-electron potential redox capacity [1]. More than that, due to large ionic channels, PB able to cater large and wide variety cation with ease such as Li^+ Na^+ and K^+ to be inserted and deinserted [2]. The Prussian blue (PB) and its analogs ($A_2M[Fe(CN)_6]$ M=Fe, Co, Mn, Ni, Cu, etc) has a cubic crystalline framework (space group = Fm$\underline{3}$m) [3] can be easily synthesized using simple precipitation method by reacting transition metal cation (Mn^+) with anion ($Fe(CN)_6$)[4–6].

To achieve good electrochemical performance, high quality PBAs with a low defect and high crystallinity are demanded. Goodenough *et al.* [7] has performed an effective method to regulate chemical precipitation of KMHCF by slowing down the nucleation and grain growth. This method improves the crystallinity of structure and reduces the amount of $Fe(CN)_6$ vacancies which in turn reduce the water content. This cathode shows excellent cycling stability at 100% and 80% capacity after 200 and 1000 cycles respectively.

*Corresponding author: *fadhlul@upnm.edu.my*, *mfariz@uitm.edu.my*

Jing Song *et al.* [7] in their work has removed the interstitial water in $Na_2Mn[Fe(CN)_6].zH_20$ shows a high reversible capacity at 3.5 V with excellent rate and cycling performance which retain 75% of capacity after 500 cycles. Xianyong *et al.* [8] synthesis low defect $FeFe(CN)_6$ using facile hydrolytic precipitation. High performance cathode has been obtained due to nearly perfect structural and minimized lattice water with the capacity of 160 mAh g^{-1} at 24 C and able to retain 90% after 300 cycles.

In this present work, the effect of water toward the structural and electronic properties of Prussian Blue cathode material is investigated using Density Functional Theory (DFT) approach. The $Fe(CN)_6$ vacancy is introduced and water molecules were added to the structure. The existence of water molecules in PB complicates their structural, electronic and electrochemical properties. As an example, Song et al. [9] have reported that the existence of water molecules (H_2O) in PB in $Na_2MnFe(CN)_6$ cathode not only affects its crystal structure but also changes the shape of it voltage profile. The influence of water molecules (H_2O) in PB was found to have a profound influence on the bandgap and density of states of this material. The result of the lattice parameter, bandgap, density of state and charge density reports and discussed. The result then will be compared with the stochiometric structure of Prussian Blue.

2. METHODS

In this study, the calculations were performed using the CASTEP computer code [10] using LDA, GGA-PBE and GGA-PBEsol exchange-correlation functional. The convergence test for cut-off and *k*-point size was performed prior to geometry relaxation. The PB crystal structure was constructed base on the atomic position data in Table 1 using Material Studio Visualizer. Due to the limitations of DFT which normally underestimate the electronic calculation of the strongly corelated material, GGA + U method was used to correct the problem. The GGA + U was first invented by Anisimov and Gunnarson then translated into viable computational methodology by various researchers [11]. Spin polarized were considered. The energy cut-off was set at 380 eV and 6×6×6 *k*-point. From the previous research, the value of U was determined using a systematic scan through a wide range of U values and considering both structural and electronic properties of the obtained solutions and the optimum value of U obtained were U=3.0 eV and U=7.0 eV for Fe^{2+} and Fe^{3+} sites respectively for Prussian Blue [12]. For the insertion of water molecules into Prussian Blue, the calculations were performed using GGA+U functionals with 380 eV for cut-off energy and 4×4×4 *k*-point. The crystal structure of pure Prussian Blue and hydrated Prussian Blue as shown in Figure 1.

Table 1 Atomic position, space group and lattice parameter for Prussian Blue [13]

Space group = $Fm\underline{3}m$, a = 10.218 Å			
Atoms	***x***	***y***	***z***
Fe_1	0	0	0
Fe_2	0.5	0.5	0.5
C	0.312	0	0
N	0.196	0	0
H_2O	0.331	0.331	0.331

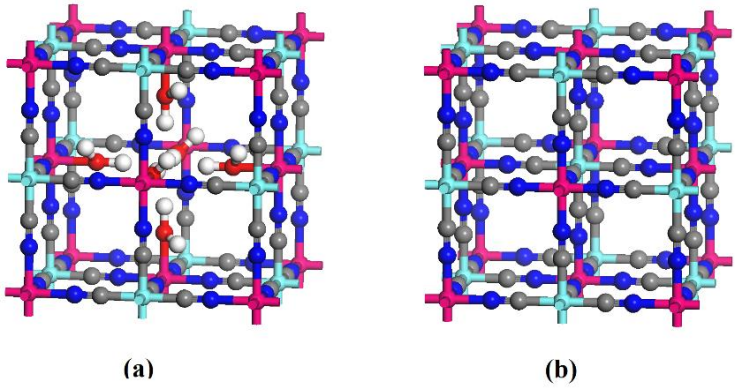

Figure 1. The crystal structure of (a) hydrated and (b) pure Prussian Blue. The grey, blue, light blue, magenta, red and white represent carbon, nitrogen, Fe (low spin), Fe (high Spin), oxygen and hydrogen atom respectively.

3. RESULTS AND DISCUSSION

Prior to the geometrical optimization, the convergence test (Figure 2) is performed by running total energy with respect to cut-off energy and *k*-point. The *k*-point is set to constant while varying the cut-off and vice-versa. The cut-off energy and *k*-point is varying from 100 to 500 eV and 1×1×1 to 9×9×9 respectively. As can be seen in Figure 2(a), the highest total energies are observed at 100 eV and start to converge at 300 eV. On the other hand, *k*-point start to converge at 6×6×6 as seen in Figure 2(b). These cut-off energies and *k*-point selection are to ensure the accuracy of the calculations of Prussian Blue with an appropriate computational cost.

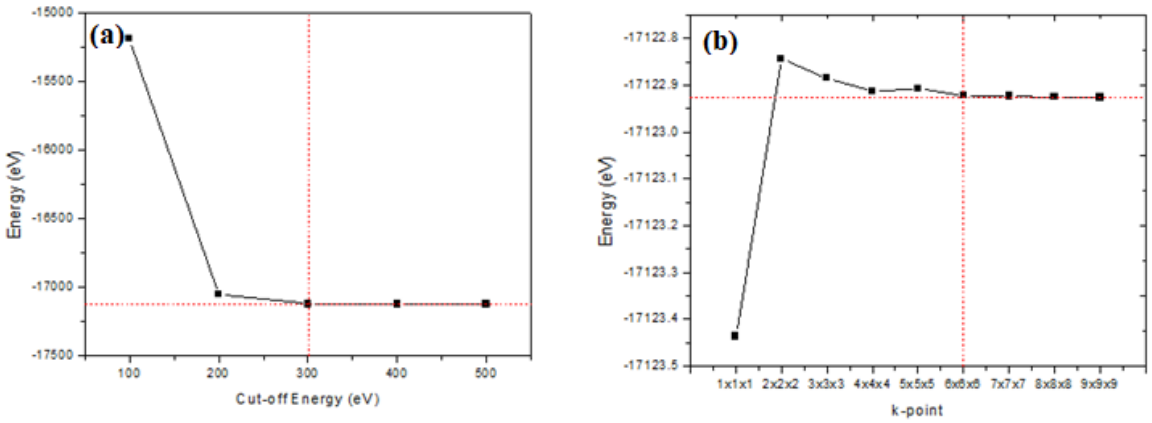

Figure 2. The convergence test with respect to (a) cut-off energy and (b) k-point.

Table 2 shows the calculation of lattice parameters, volume, bandgap, bond length and (bond order) of the pure and hydrated Prussian Blue by using different functions. For pure PB, the lattice parameters calculated using both LDA and GGA-PBEsol functionals show some underestimated and overestimated value compared to the experimental works [14] which are -1.35% and 4.75% respectively. Meanwhile for GGA-PBE functional, only 0.03% lattice parameter deviation which is in good agreement with experimental work. Thus, for hydrated PB, GGA-PBE is used to calculate the lattice parameter. From bond order (BO) value, the type of the bond between two atoms can be determined. Normally, for a single bond the BO will range from 0 to 1 which the more it approaches 0, the more ionic character it is and the more it approaches 1 the more covalent character it is. As shown in Table 2, BO for the three functional is almost the same. For GGA-PBE, the BO of Fe-C and Fe-N were in the range of 0.16 until 0.21. These show that these

two bonds are covalent bonded. For C-N bond, the BO is 1.80 and it is the highest BO because it is the shortest and triple bond in nature.

It can be seen that, the geometry framework between of pure Prussian Blue and hydrated Prussian Blue are slightly different. Upon removing of $Fe(CN)_6$ and introduction of water molecules into the cavity of Prussian Blue, the structure undergoes a slight contraction and distorted from the ideal cubic cell as can be seen in Figure 3. The lattice parameter slightly reduced compared to the pure Prussian Blue by about 0.3 Å. From the BO results, the Fe-C bond still the same (0.16) as the pure Prussian Blue while C-N bond not much different from the pure Prussian Blue. For Fe-N bond, the BO (0.1) is lower compare to Fe-N in pure PB. This is the sign of weaker bond which can lead to a fragile framework and tends to collapse during charge/discharge thus lead to poor cycle life [1].

Without GGA + U the generated bandgap for pure Prussian Blue is 0.3 eV (Table 2). Compare with the experimental result (1.75 eV), this discrepancy is due to the GGA exchange correlation tend to produce underestimated electronic band gap which arising from the incomplete cancellation of the Coulomb self-interaction between localized transition metal 3d electron [15,16] . After the addition of Hubbard U term, the electronic band gap rises to 1.66 eV which is in good agreement with the experimental result.

Table 2 Calculated of lattice parameters, volume, bandgap, bond length and (bond order) of the pure and Hydrate Prussian Blue by using different functional

	Functional	GGA-PBE	GGA-PBEsol	LDA-CAPZ	GGA-PBE+U	Theoretical	Experiment
Pure Prussian blue	$a = b = c$ (Å)	10.197	10.062	9.715	10.216	10.246 [17] 9.910 [12] 10.140 [18] 10.260 [19]	10.200 [14]
	V (Å^3)	1060.313	1018.702	916.940	1066.209		
	ΔE_g (eV)	0.300			1.660		1.75 [20]
Hydrated Prussian Blue	$a = b = c$ (Å)	9.912	-	-	-	-	-
	V (Å^3)	970.600	-	-	-	-	-
	ΔE_g (eV)	-	-	-	1.033	0.6 [21]	-

Bond length (Bond Order) of Pure Prussian Blue				Bond length (Bond Order) of Hydrated Prussian Blue			
	GGA-PBE	GGA-PBEsol	LDA-CAPZ		GGA-PBE	GGA-PBEsol	LDA-CAPZ
Fe-N	2.023 (0.21)	1.863 (0.24)	1.839 (0.23)	Fe-N	1.889 (0.10)	-	-
Fe-C	1.887 (0.16)	1.865 (0.19)	1.841 (0.18)	Fe-C	1.880 (0.16)	-	-
C-N	1.189 (1.80)	1.186 (1.86)	1.177 (1.88)	C-N	1.184 (1.82)	-	-
				Fe-O	1.980 (0.03)	-	-
				H-O	0.971 (0.31)	-	-

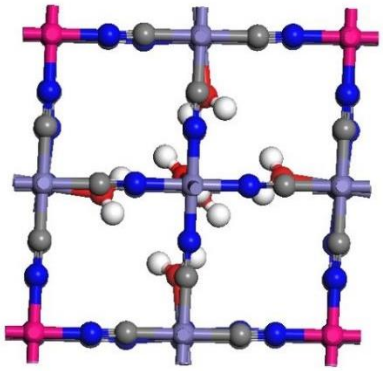

Figure 3. Distorted structure of hydrated Prussian Blue. The angle, α = 92.67°.

For hydrated PB, the bandgap obtained is 1.03 eV which is lower compare to pure PB as shown in Figure. 4. The band structure of hydrated PB and pure PB are remarkably different. This is due to the $Fe(CN)_6$ vacancies and water molecules have induced the change in the electronic properties of PB [6]. Compare to other theoretical calculations, which can be found in work by Wodjel [21], this work overestimated about ~0.4 eV. However, the result still in agreement with each other. Water molecules (H_2O) induced change is accompanied by the appearance of dispersing low laying unoccupied bands, instead of the narrow band in pure PB.

In Figure 5, shows that the partial density of states (pDOS)for both hydrated PB and pure PB. For partial density of states (pDOS) of hydrated PB, shows that Fe 3*d* orbital is the most contributed in both valence band and conduction band while C 2*p* orbital highly contribute in conduction band. In addition, O *2s* orbital contributed on the upper and lower valence band. Same goes as pure PB, it can be seen that the conduction and valance band are mostly contributed by the Fe 3*d* orbital. For the upper conduction band, most of the contribution come from N 2*p* and C 2*p* orbital and same goes to the lower valance band. The shape of pDOS of N 2*p* and C 2*p* are only slightly different and fully overlap. This phenomenon might be due to the strong triple bonding between C and N atom. This phenomenon might be due to the strong triple bonding between C and N atom. Additionally, this feature important to maintain structure rigidity and prolong the cycle life of the battery [22]. Fe 3*d* orbital does not form narrow band in pure PB. Low ligand strength of the water molecule presented in hydrated PB responsible for the broader splitting of unoccupied *d* orbitals energy and consequently narrowing of the band gap significant. This present works show that the band gap of hydrated PB is lower than pure PB is in agreement with previous report obtained from ligand-field theory for $KFe[Co(CN)_6]$ PB analogue [23]. Due to this fact, the hydrated PB is predicted to have better electronic conductivity at finite temperature [21]. Even though the electronic conductivity is increased, the present of water molecule is associated with the reducing amount of sodium insertion capacity and lower Na+ migration kinetic [24].

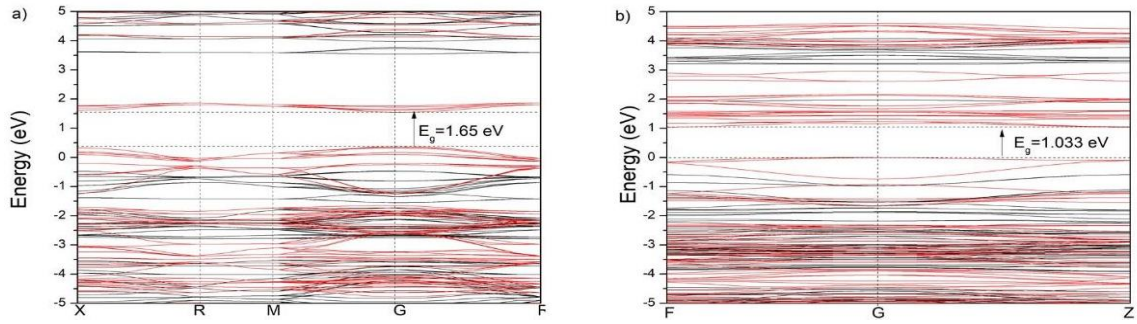

Figure 4. Band structure of (a) pure PB with exchange correlation GGA-PBE+U at (Fe^{3+}:U=7 eV and Fe^{2+}:U=3 eV) and (b) hydrated PB.

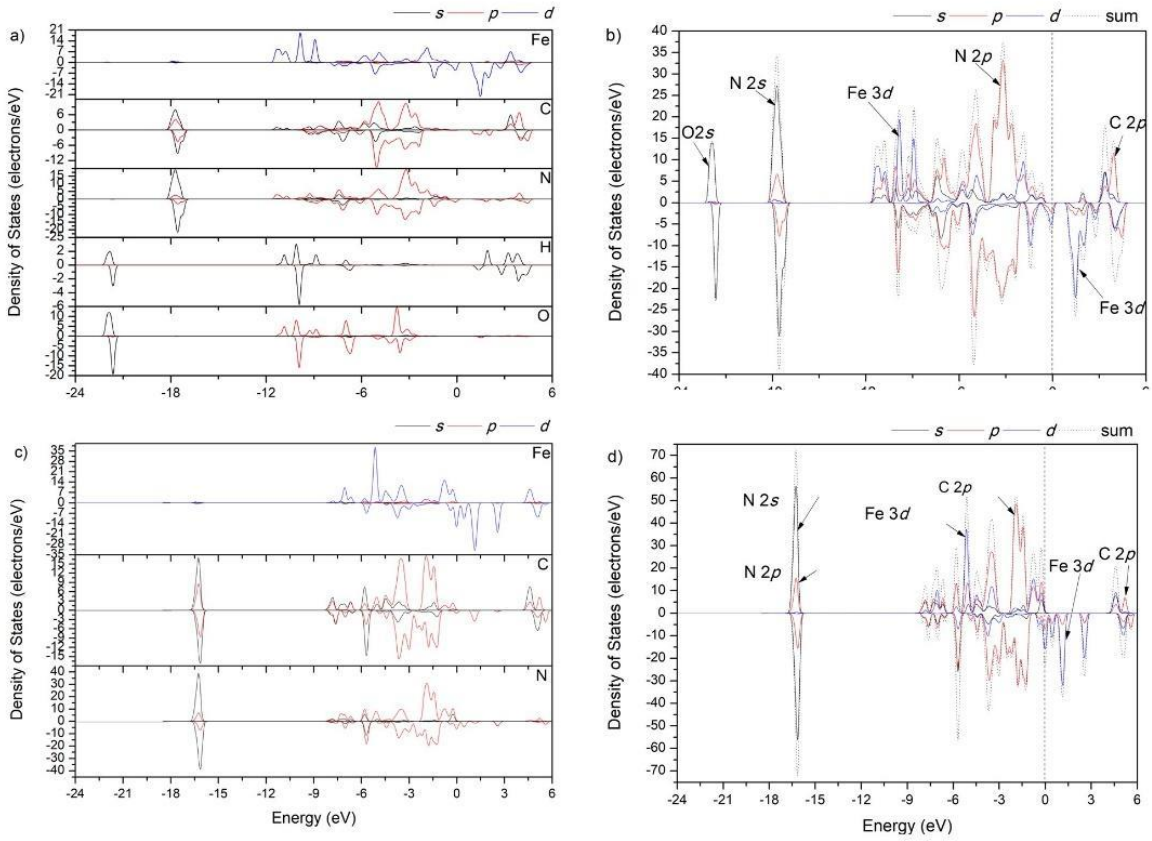

Figure 5. Calculated (a) partial density of states (pDOS) of hydrated PB, (b) atom projected sum DOS for hydrated PB, (c) partial density of states (pDOS) of pure PB and (d) atom projected sum DOS for pure PB.

From Figure 6, the electron distribution and chemical bonding nature of hydrated PB can be further understood from the plots of electron density map with the ranges of the field density (blue to red indicates a change in electron density from low to high where 0 represent fully ionic and 2 represent fully covalent). The most obvious density can be seen between C-N bond as they are triple bonded. This support the Density of State and Bond Order result which indicate strong covalent character between then. Meanwhile for Fe-N, Fe-C, O-H and Fe-O bond, a significant amount of density can be seen which also indicate covalent character. Overall, compare to pure PB charge density, only slightly different can be notice.

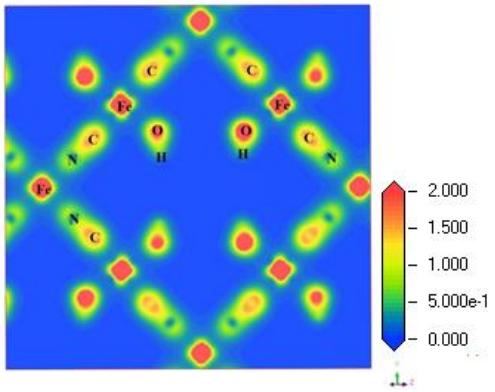

Figure 6. Charge-density diagram of Hydrated Prussian Blue.

The water molecules (H_2O) show the wetting properties such as hydrophobicity and hydrophilicity determined by water-substrate interactions [23, 24]. Other than that, the hydrogen

bonds (H-bonds) can form through the binding and collision of water molecules (H_2O) with other host in which are comparable in strength to the adsorption interactions of water molecules on substrate and it called as physisorption or chemisorption [27]. To evaluate the stabilities of the water molecules (H_2O) adsorbed on PB, we used the following equation for the adsorption energy

$$E_a = E\left(\left(\frac{(H_2O)_n}{PB}\right) - E(H_2O)_n - E(PB)\right) \quad (1)$$

where the equation represents the total energy after optimization for water molecules (H_2O) adsorption on vacancy PB crystal structure. The chemisorption energy of water adsorption to the crystal structure PB 0.182 meV per H-bond respectively. The positive value means the adsorption is supposed to be repulsive although the value is very small. However, it common to for synthesised PB to contain small amount of parasitic coordinated water, depend on the method of synthesis [28]. Song et al. able to prepare good quality and performance by synthesised PB cathode material with ignorable water content [29]. Thus, by finding the right way of synthesis, this parasitic water will be diminished thus improving the quality and performance of this cathode material.

4. CONCLUSION

From the first principles calculation, $Fe(CN)_6$ vacancies and water filled cavities in the Prussian Blue gave a drastic change in the electronic structure of this material. Even though the band gap was lowered compared to the pure Prussian Blue cathode material, present of water still hindered the electrochemical performance. The structure of hydrated Prussian blue is shrinking, weaken and distorted from the ideal cubic structure can cause the performance of Prussian Blue cathode material to drop as the structure tend to collapse. The C-N bond play important role in the structure rigidity as it possesses highest Bond Order which important to endure for long cycle life. All the result from Bond order, Density of State and Charge Density are supporting each other's. Eventually, when it comes to synthesis this material, it is important to reduce the $Fe(CN)_6$ vacancies inside the cathode material in order to get high performance PB cathode material. Base on positive adsorption energy, water molecules are expected to be repulsive toward PB even though the value is almost zero. Most of the high quality PB will have low concentration of water content inside the structure.

ACKNOWLEDGEMENTS

This work is supported by internal UPNM grant (Grant code: UPNM/2018/GPJP/2/SG/3). The authors would like to express their gratitude to Institute of Science's Ionic Materials & Devices (i-MADE) Lab, in Faculty of Applied Science, UiTM for their support in providing research facilities to carry out this research.

REFERENCES

[1] Wu, X., Wu, C., Wei, C., Hu, L., Qian, J., Cao, Y., Ai, X., Wang, J., Yang, H., ACS Appl. Mater. Interfaces. **8**, 8 (2016) 5393–5399.
[2] Phadke, S., Mysyk, R., Anouti, M., J. Energy Chem. **40** (2019) 31–38.
[3] Ling, C., Chen, J., Mizuno, F., J. Phys. Chem. C. **117**, 41 (2013) 21158–21165.
[4] Xie, M., Xu, M., Huang, Y., Chen, R., Zhang, X., Li, L., Wu, F., Electrochem. Commun. **59** (2015) 91–94.

[5] Li, W. J., Chou, S. L., Wang, J. Z., Wang, J. L., Gu, Q. F., Liu, H. K., Dou, S. X., Nano Energy. **13** (2015) 200–207.
[6] Yang, Y., Liu, E., Yan, X., Ma, C., Wen, W., Liao, X.-Z., Ma, Z.-F., J. Electrochem. Soc. **163**, 9 (2016) A2117–A2123.
[7] Zhou, A., Xu, Z., Gao, H., Xue, L., Li, J., Goodenough, J. B., Small. **15**, 42 (2019) 1–6.
[8] Wu, X., Leonard, D. P., Ji, X., Chem. Mater. **29**, 12 (2017) 5031–5042.
[9] Xiao, P., Song, J., Wang, L., Goodenough, J. B., Henkelman, G., Chem. Mater. **27**, 10 (2015) 3763–3768.
[10] Kresse, G., Furthmu, J. **54**, 16 (1996).
[11] Anisimov, V. I.; Gunnarsson, O. **43**, 10 (1991).
[12] Wojdeł, J. C., De P. R. Moreira, I., Bromley, S. T., Illas, F., J. Chem. Phys. **128**, 4 (2008).
[13] Kumar, A., Yusuf, S. M., Keller, L., Phys. Rev. B - Condens. Matter Mater. Phys. **71**, 5 (2005) 1–7.
[14] Ojwang, D. O., Grins, J., Wardecki, D., Valvo, M., Renman, V., Häggström, L., Ericsson, T., Gustafsson, T., Mahmoud, A., Hermann, R. P., Svensson, G., Inorg. Chem. **55**, 12 (2016) 5924–5934.
[15] Husin, R., Badrudin, F. W., Taib, M. F. M., Yahya, M. Z. A., Mater. Res. Express. **6**, 11 (2019) 114002.
[16] Badrudin, F. W., Taib, M. F. M., Mustapha, R. I. P. R., Hassan, O. H., Yahya, M. Z. A., Mater. Today Proc. **4**, 4 (2017) 5108–5115.
[17] Hegner, F. S., Galán-Mascarós, J. R., López, N., Inorg. Chem. **55**, 24 (2016) 12851–12862.
[18] Fan, L., Liu, Q., Xu, Z., Lu, B., ACS Energy Lett. **2**, 7 (2017) 1614–1620.
[19] Targholi, E., Mousavi-Khoshdel, S.M., Rahmanifara, M., Yahya, M. Z. A., Chem. Phys. Lett. **687** (2017) 244–249.
[20] Robin, M.B., Inorg. Chem. **1**, 2 (1962) 337–342.
[21] Wojdeł, J. C., J. Mol. Model. **15**, 6 (2009) 567–572.
[22] Badrudin, F. W., Taib, M. F. M., Hassan, O. H., Yahya, M. Z. A., Comput. Mater. Sci. vol **119**, (2016) 144–151.
[23] Kawamoto, T., Asai, Y., Abe, S., Phys. Rev. B. **60**, 18 (1999) 12990–12993.
[24] Wu, X., Deng, W., Qian, J., Cao, Y., Ai, X., Yang, H., J. Mater. Chem. A. **1**, 35 (2013) 10130–10134.
[25] Henderson, M. A., London, A., York, N., Paris, O., Tokyo, S., (n.d.).
[26] Verdaguer, A., Sacha, G. M., Bluhm, H., Salmeron, M., (2006) 1478–1510.
[27] Hu, W., Li, Z., Yang, J., **2** (2016) 1–11.
[28] Xie, B., Zuo, P., Wang, L., Wang, J., Huo, H., He, M., Shu, J., Li, H., Lou, S., Yin, G., Nano Energy. **61**, April (2019) 201–210.
[29] Song, J., Wang, L., Lu, Y., Liu, J., Guo, B., Xiao, P., Lee, J. J., Yang, X.Q., Henkelman, G., Goodenough, J. B., J. Am. Chem. Soc. **137**, 7 (2015) 2658–2664.